British Journal of Pharmacology

RESEARCH PAPER

PF-06526290 can both enhance and inhibit conduction through voltage-gated sodium channels

Correspondence Neil A. Castle, Work, Pfizer Inc. (currently Icagen Inc.), 4222 Emperor Boulevard, Durham, NC 27703, USA. E-mail: ncastle@icagen.com

Received 14 November 2017; **Revised** 6 March 2018; **Accepted** 17 March 2018

Lingxin Wang[1], Shannon G Zellmer[2], David M Printzenhoff[2] and Neil A Castle[2]

[1]Department of Molecular and Cellular Physiology, Stanford University, Stanford, CA, USA, and [2]Icagen Inc., Durham, NC 27703, USA

BACKGROUND AND PURPOSE

Pharmacological agents that either inhibit or enhance flux of ions through voltage-gated sodium (Na_v) channels may provide opportunities for treatment of human health disorders. During studies to characterize agents that modulate $Na_v1.3$ function, we identified a compound that appears to exhibit both enhancement and inhibition of sodium ion conduction that appeared to be dependent on the gating state that the channel was in. The objective of the current study was to determine if these different modulatory effects are mediated by the same or distinct interactions with the channel.

EXPERIMENTAL APPROACH

Electrophysiology and site-directed mutation were used to investigate the effects of PF-06526290 on Na_v channel function.

KEY RESULTS

PF-06526290 greatly slows inactivation of Na_v channels in a subtype-independent manner. However, upon prolonged depolarization to induce inactivation, PF-06526290 becomes a Na_v subtype-selective inhibitor. Mutation of the domain 4 voltage sensor modulates inhibition of $Na_v1.3$ or $Na_v1.7$ channels by PF-06526290 but has no effect on PF-06526290 mediated slowing of inactivation.

CONCLUSIONS AND IMPLICATIONS

These findings suggest that distinct interactions may underlie the two modes of Na_v channel modulation by PF-06526290 and that a single compound can affect sodium channel function in several ways.

Abbreviations

DRG, dorsal root ganglion; Na_v, voltage-gated sodium; PF-06526290, N-benzyl-N-methyl-4-(3-(thiazol-2-yl)ureido) benzenesulfonamide; VSD, voltage sensor domain

DOI:10.1111/bph.14338

Introduction

Voltage-gated sodium (Na_v) channels are critical for the initiation and propagation of action potentials in electrically excitable cells (Hodgkin and Huxley, 1952; Bezanilla, 2006; Catterall, 2012). In mammals, there are nine Na_v channel subtypes that can have broad or highly localized tissue expression distribution, which enables them to serve distinct physiological functions such as neuronal electrical signalling, neurotransmitter release, cardiac and skeletal muscle contraction and non-excitatory roles (Cummins *et al.*, 2007; Catterall, 2012; Black and Waxman, 2013). The importance of Na_v channels in these physiological processes is highlighted by numerous reports of human Na_v genetic channelopathies associated with pain, epilepsy, autism, cardiac arrhythmias and skeletal muscle myotonias (Catterall, 2012; Eijkelkamp *et al.*, 2012; Bennett and Woods, 2014; Krumm *et al.*, 2014; Miller *et al.*, 2014; Moreau *et al.*, 2014; Waxman *et al.*, 2014). Because of this association, pharmacological modulation of sodium channel function has been a primary mode of clinical intervention to treat many of these disorders. Therefore, there is considerable interest in developing Na_v subtype-selective drug candidates (England and de Groot, 2009). Much of the recent focus and success has been in the identification and development of selective inhibitors of **$Na_v1.8$**, **$Na_v1.3$** and **$Na_v1.7$** sodium channel subtypes (Jarvis *et al.*, 2007; Kort *et al.*, 2008; Zhang *et al.*, 2010; McCormack *et al.*, 2013; Lee *et al.*, 2014; Sun *et al.*, 2014; Ahuja *et al.*, 2015; Bagal *et al.*, 2015; Payne *et al.*, 2015; Alexandrou *et al.*, 2016). However, recent reports that human **$Na_v1.1$**, **$Na_v1.2$**, $Na_v1.3$ and **$Na_v1.6$** channel loss of function mutations can lead to seizure disorders and some forms of autism have increased interest in potentially developing drug candidates that can enhance Na_v channel activity (Jensen *et al.*, 2014; Blanchard *et al.*, 2015; Crestey *et al.*, 2015; Lamar *et al.*, 2017; Wolff *et al.*, 2017)

Development of selective small molecule Na_v channel inhibitors was recently aided by the identification and characterization of a novel pharmacological interaction region on the homologous domain 4 voltage sensor of the channel (McCormack *et al.*, 2013; Ahuja *et al.*, 2015). This region is distinct from the more well characterized local anaesthetic binding site located within the pore of the channel (Ragsdale *et al.*, 1994; Ragsdale *et al.*, 1996; Fozzard *et al.*, 2011; Panigel and Cook, 2011), which is believed to be the site of interaction for many of the clinically used non-selective Na_v channel modulators. The homologous domain 4 voltage sensor is also the site of interaction of venom peptide toxins from scorpions, sea anemones and wasps that enhance conduction of Na_v channels *via* a slowing of the inactivation process (Leipold *et al.*, 2004; Gilchrist *et al.*, 2014). Many of these toxins exhibit Na_v channel subtype selectivity which suggests that the homologous domain 4 voltage sensor may be an attractive target for the development of selective low MW enhancers of Na_v channel conduction. In the current study, we describe the characterization of a novel compound PF-06526290 identified during a screen of compounds that had some structural relationship to the selective aryl sulfonamide class of inhibitors previously shown to interact with the homologous domain 4 voltage sensor (McCormack *et al.*, 2013; Ahuja *et al.*, 2015). This novel Na_v channel modulator exhibits both enhancement and inhibition of Na_v channels function and that the divergent functions may result from distinct interactions with the channel that may include the homologous domain 4 voltage sensor region.

Methods

Cell line generation/isolation

Human $Na_v1.3$, $Na_v1.7$, $Na_v1.3$ M123-S1510Y/R1511W/E1559D and $Na_v1.7$ M123-Y1537S/W1538R/D1586E channels were stably expressed in HEK293 cells. **$K_v1.1/K_v1.2$** (heteromultimer) channels were stably expressed in CHO cells. Methods of stable cell line generation were as described in McCormack *et al.* (2013). Mouse dorsal root ganglion (DRG) neurons were isolated as described by Gandini *et al.* (2014).

Electrophysiology

Studies were performed using conventional or automated whole-cell patch clamp electrophysiology. Extracellular recording solution contained 138 mM NaCl, 2 mM $CaCl_2$, 5.4 mM KCl, 1 mM $MgCl_2$, 5 mM glucose and 10 mM HEPES, pH 7.4 with NaOH. For DRG neuron voltage-clamp recordings sodium concentration was reduced to 40 mM (i.e. 98 mM choline chloride substituted for NaCl) while remaining constituents were unchanged. Internal (intracellular) recording solutions for sodium current contained 110 mM CsF, 35 mM CsCl, 5 mM NaCl, 5 mM EGTA and 10 mM HEPES pH 7.4 with CsOH (KF replaced CsF for potassium current recording). Recordings were performed at room temperature using AXOPATCH 200B amplifier and pCLAMP software or PatchXpress 7000 (Molecular Devices). Peak current amplitudes ranging 2–10 nA were used for characterization of our compounds. Voltage errors were minimized using 80% series resistance compensation.

Test agents were made up as 10 mM DMSO stock solutions and diluted in extracellular solution to attain final concentrations desired. The final concentration of DMSO (<0.3%) had no effect on recorded current properties. Toxin stock solutions were made at 100 μM in the extracellular recording solution and stored at −20°C. Before use, stock solution was diluted in recording solution containing 0.1% of bovine serum albumin. All reagents were applied to cells *via* a parallel pipe perfusion system (Castle *et al.*, 2003). Experimental protocols and test agent were not randomized because, for the most part, only one compound and one experimental protocol was evaluated on an individual cell. All compound testing followed a control measurement period.

For current-clamp recordings, pipette solution contained the following: 140 mM K-Aspartate, 10 mM KCl, 8 mM NaCl, 20 μM EGTA, 10 mM HEPES, 1 mM $MgCl_2$, 2 mM Mg-ATP and 0.4 mM Na-GTP, pH 7.4 with KOH; and the bath solution contained 138 mM NaCl, 2 mM $CaCl_2$, 5.4 mM KCl, 1 mM $MgCl_2$, 5 mM glucose and 10 mM HEPES, pH 7.4 with NaOH. Action potential current threshold was determined by the first action potential elicited by a series of depolarizing current injections (30 ms) from 10 pA with 10 pA increments. Action potential frequency was determined by quantifying

the number of action potentials elicited in response to 500 ms 150 pA current injections.

Data and statistical analysis

Data and statistical analysis comply with the recommendations on experimental design and analysis in pharmacology (Curtis *et al.*, 2015). Electrophysiological data were analysed using Clampfit 10.3 (Molecular Devices) and GraphPad Prism 6.0 (GraphPad Software, Inc., San Diego, CA, USA). Statistical analysis of data was performed using Student's *t*-test or ANOVA where appropriate. Statistical significance was set at $P < 0.05$. All data are presented as individual data points and/or mean values ± SEM.

Materials

PF-06526290 was synthesized by the medicinal chemistry group at Pfizer. Scorpion α-like toxin Lqh III was purchased from Latoxan, France, and **tetrodotoxin** (TTX) was bought from Sigma Aldrich.

Nomenclature of targets and ligands

Key protein targets and ligands in this article are hyperlinked to corresponding entries in http://www.guidetopharmacology.org, the common portal for data from the IUPHAR/BPS Guide to PHARMACOLOGY (Harding *et al.*, 2018), and are permanently archived in the Concise Guide to PHARMACOLOGY 2017/18 (Alexander *et al.*, 2017).

Results

PF-06526290 slows Na_v channel inactivation

The compound, PF-06526290 (Figure 1A), was identified during a screen for novel $Na_v1.3$ channel inhibitors. In contrast to inhibition, the most noticeable effect of PF-06526290 was a slowing of the rate of $Na_v1.3$ current inactivation. Figure 1 B shows that depolarization from −120 to 0 mV in the presence of 10 μM PF-06526290 resulted in activation of $Na_v1.3$ currents that exhibited greatly slowed inactivation compared to non-treated controls [τ_{inact} (control) = 0.82 ± 0.04 ms, n = 15 vs. τ_{inact} (PF-06526290) = 96 ± 9 ms, n = 6]. Figure 1C shows that 10 μM PF-06526290 produces a similar slowing of inactivation of human $Na_v1.7$ currents. The concentration dependence of slowing of inactivation (Figure 1D) was determined by normalizing the current amplitude 5 ms after start of depolarizing voltage step in the presence and absence of PF-06526290 to peak sodium current amplitude. The EC_{50}s are 1.1 ± 0.1 μM (n = 6) for $Na_v1.3$ and 0.27 ± 0.08 μM (n = 5) for $Na_v1.7$ channels. Maximal slowing of $Na_v1.7$ inactivation with 10 μM PF-06526290 occurred within 2 min, and

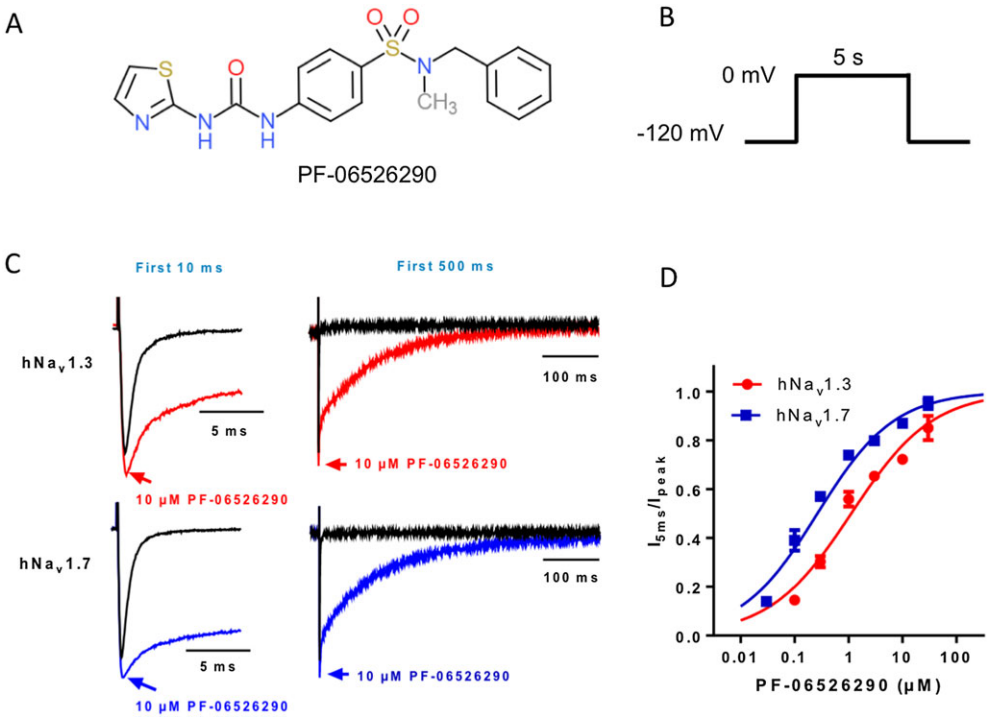

Figure 1

PF-06526290 slows Na_v channel inactivation. (A) Structure of PF-06526290. (B) Voltage protocol employed to evaluate PF-06526290 effect on sodium channel function. (C) Current traces for the first 10 ms (left) or 500 ms (right) of the 5 s voltage step to 0 mV, showing the effect of PF-06526290 on human $Na_v1.3$ and $Na_v1.7$ channel activity. (D) Concentration dependence of human $Na_v1.3$ and $Na_v1.7$ slowed inactivation following PF-06526290 treatment. Magnitude of PF-06526290-induced slowing of inactivation was calculated by normalizing sodium current amplitude 5 ms after peak-to-peak amplitude; EC_{50} 0.27 ± 0.08 μM (n = 5) for $Na_v1.7$ and 1.1 ± 0.1 μM (n = 6) for $Na_v1.3$ channels. Data values for $Na_v1.7$ channels derived from 21 cells from nine separate cell preparations. Data values for $Na_v1.3$ channels derived from 20 cells from eight separate cell preparations.

more than 80% of this effect could be reversed by washout for 10 min (Figure 2A). We investigated the possibility that β1 and β2 auxiliary subunits coexpressed with $Na_v1.7$ channels might modulate slowing of inactivation produced by PF-06526290. However, no effect was observed (Figure 2B, C).

Figure 3A shows that slowing of inactivation by PF-06526290 was observed for all Na_v channels subtypes evaluated, although the magnitude of effect at 10 μM was noticeably less for human **$Na_v1.4$** and $Na_v1.8$ channels. The quantification of inactivation slowing (I_{5ms}/I_{Peak} ratio) for each of the channel subtypes is summarized in the plot in Figure 3B.

Figure 4A, B shows the peak current amplitude versus stimulating voltage relationship for $Na_v1.3$ and $Na_v1.7$ channels in the absence and presence of 10 μM PF-06526290. For both channel subtypes, there was a PF-06526290-associated increase in peak current amplitude at voltages near the activation threshold. Figure 4C, D shows that PF-06526290 produced a hyperpolarizing shift in voltage dependence of activation for both $Na_v1.3$ and $Na_v1.7$ channels and a larger depolarizing shift in voltage dependence of inactivation. At sub-maximal effective concentrations of PF-06526290, the voltage dependence of inactivation of $Na_v1.7$ channels exhibited a double Boltzmann voltage relationship, which could be fit with two midpoint inactivation potentials and slopes equal to either control (−70 mV) or 10 μM compound (−32 mV). However, the relative proportion of the depolarized midpoint potential component (i.e. −32 mV) increased with higher PF-06526290 concentrations (Figure 4E) suggesting that this reflects the voltage dependence of inactivation of modified channels.

Multiple modes of modulation of Na_v channels by PF-06526290

The ability of PF-06526290 to slow current inactivation when activated from −120 mV suggests that the compound interacts with the channel in a closed resting state. Although PF-06526290 slows Na_v channel inactivation, it does eventually reach completion. This allowed for the evaluation of compound interaction with inactivated $Na_v1.3$ and $Na_v1.7$ channels. Figure 5A, B shows that after a 5 s conditioning voltage step to 0 mV (channels are completely inactivated for >4.5 s) followed by a 50 ms rest at −120 mV to allow

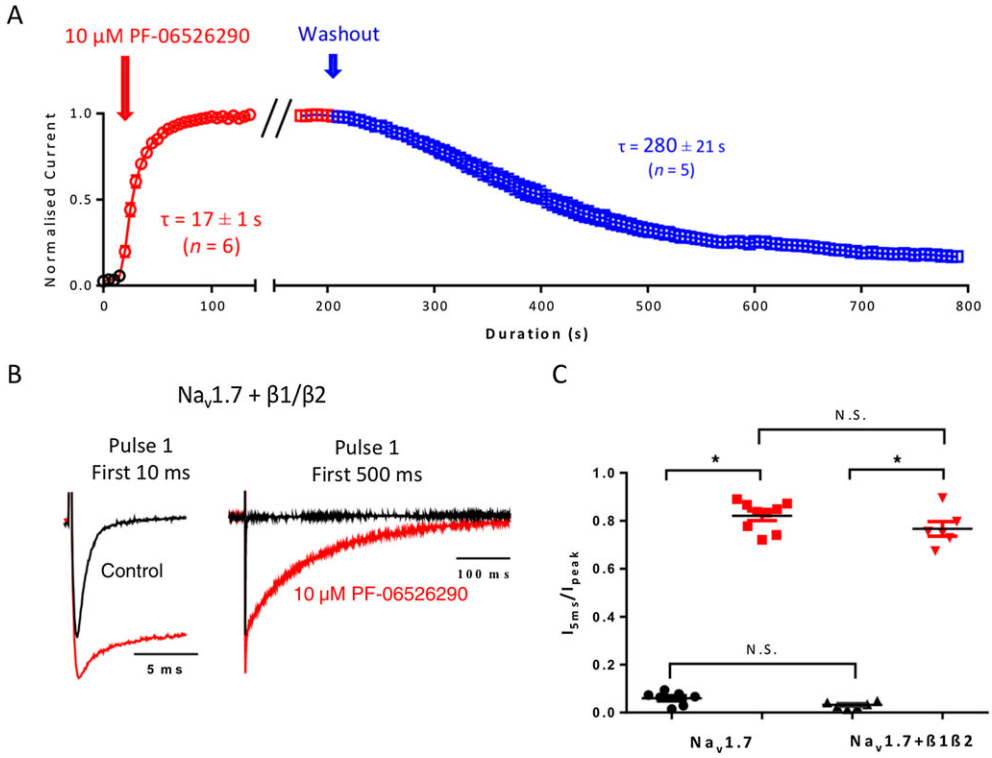

Figure 2

(A) Time course of 10 μM PF-06526290 slowing of inactivation of $hNa_v1.7$ channels and washout. Time course of $Na_v1.7$ 5 ms/peak current ratio was normalized to the maximal response in each experimental run just prior to compound washout. Data shown are mean ± SEM for five to six separate experiments. (B) Sodium channel auxiliary subunits β1 and β2 have no effects on PF-06526290 (PF-290) induced slowing of inactivation or inhibition. Representative current traces of $Na_v1.7$ + β1/β2 subunits with and without 10 μM PF-06526290 induced by a two-pulse test protocol as shown in Figure 1. (C) Co-expression of β1/β2 subunits with $Na_v1.7$ had no effect on PF-06526290 induced slowing of inactivation (I_{5ms}/I_{peak}) compared to $Na_v1.7$ α subunit only expressing cells. Individual data for $Na_v1.7$ β1/β2 from seven separate cells from two different cell preparations. Individual data for $Na_v1.7$ from nine separate cells from three different cell preparations. *$P < 0.05$, significantly different as indicated; N.S., not significant; ANOVA.

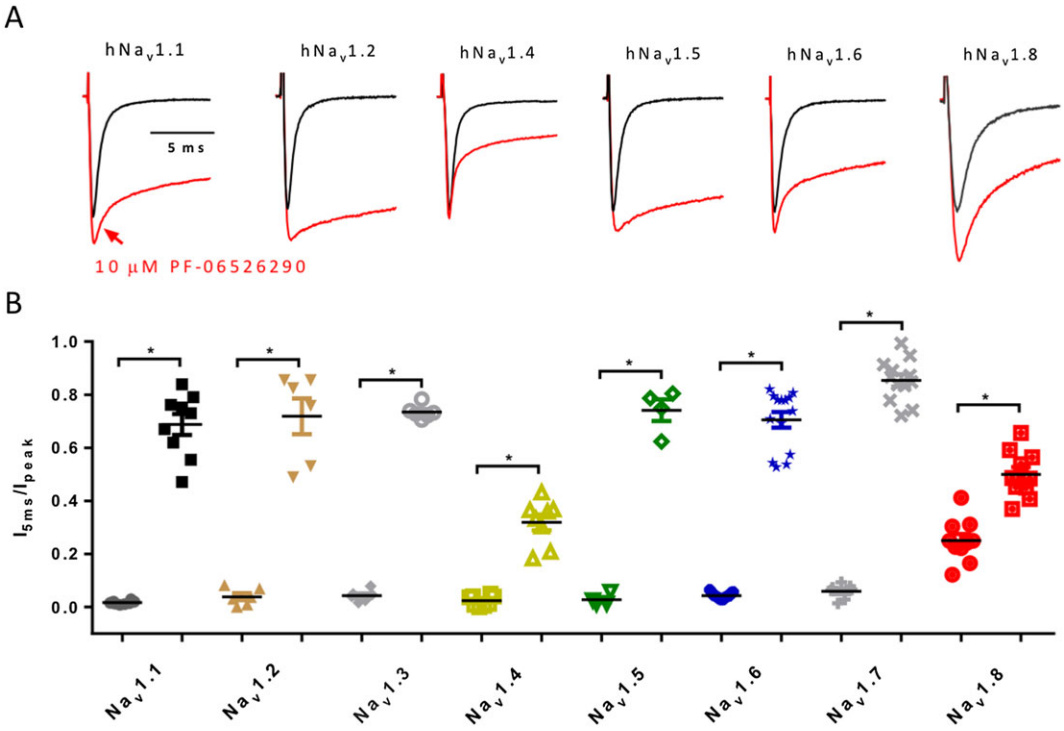

Figure 3

(A) Effect of 10 μM PF-06526290 on current amplitude and rate of inactivation of human $Na_v1.1$, $Na_v1.2$, $Na_v1.4$, $Na_v1.5$, $Na_v1.6$ and $Na_v1.8$ sodium currents elicited by Pulse 1 of the protocol illustrated in Figure 1B. (B) For each sodium channel subtype, I_{5ms}/I_{Peak} ratio before (left-hand data set) and after (right-hand data set) application of 10 μM PF-06526290 is shown. Each pair of data points for individual channel subtypes represent a separate cell recording. Data points are from 5 to 14 separate cells from two to three different cell preparations for each channel type except $Na_v1.5$ which is from four separate cells from one cell preparation. *$P < 0.05$, significantly different as indicated; *t*-test.

unmodified channels to recover from inactivation, $Na_v1.3$ but not $Na_v1.7$ currents elicited by the Pulse 2 voltage step to 0 mV were reduced by 10 μM PF-06526290. The concentration dependence of inhibition is shown in Figure 5C with the IC_{50}s being 5.1 ± 2.5 μM ($n = 6$) for $Na_v1.3$ and >30 μM ($n = 6$) for $Na_v1.7$ channels. The inhibitory effect of PF-06526290 was also observed for $Na_v1.1$, $Na_v1.6$ and **$Na_v1.5$** channels but was absent or less evident for $Na_v1.8$, $Na_v1.4$ and $Na_v1.2$ channels (Figure 5D).

PF-06526290 is functionally displaced from Na_v channel during inactivation process

An intriguing observation is that despite the absence of inhibition of $Na_v1.7$ channels by PF-06526290, currents elicited after a 5 s depolarization to 0 mV lacked the slowed inactivation seen prior to this voltage step (Figure 5A). Although not as obvious, a similar effect was observed with $Na_v1.3$ channels. If the non-inhibited component of Pulse 2 $Na_v1.3$ current in the presence of PF-06526290 is scaled to control, little or no slowed inactivation is evident (Figure 5A scaled trace). What is the explanation for this finding? One possibility is that binding of PF-06526290 and the process of inactivation are mutually exclusive, and the observed slowed inactivation reflects competition between the two processes. If this was the case, then the time course of modified inactivation would be expected to be dependent on PF-06526290 concentration. Figure 6A–C shows that time course of the slow component of inactivation is concentration independent, although the proportion of current that inactivates slowly is dependent on concentration. An alternative explanation for the concentration-independent slowing of inactivation is that PF-06526290 prevents a fast inactivation process to expose a slower inactivation process upon which the compound has no effect. Furthermore, the channel conformation associated with this slow inactivated state has a much lower affinity for PF-06526290, so it dissociates from the channel and can only rebind when the channel returns to a resting closed state. Evidence supporting this hypothesis is shown in Figure 6D–F. Figure 6D shows slowed inactivation of $Na_v1.7$ current induced by 1 μM PF-06526290 following a 20 ms voltage step from −120 to 0 mV. Figure 6E shows that when a 500 ms conditioning voltage step to 0 mV to inactivate channels is applied in the presence of 1 μM PF-06526290, followed by a 30 ms resting period at −120 mV to allow a majority of unmodified channels to recover from inactivation, currents elicited by a 20 ms voltage step to 0 mV exhibited little or no slowed inactivation. However, when the rest period at −120 mV was extended to 400 ms, ~30% of the current inactivated with slow kinetics, and when the resting period at −120 mV was further extended to 2 s, the current profile was similar to that seen in the absence of a conditioning voltage step to induce inactivation (Figure 6D, E). The rate of redevelopment of slowed inactivation increased with PF-06526290 concentration (Figure 6F).

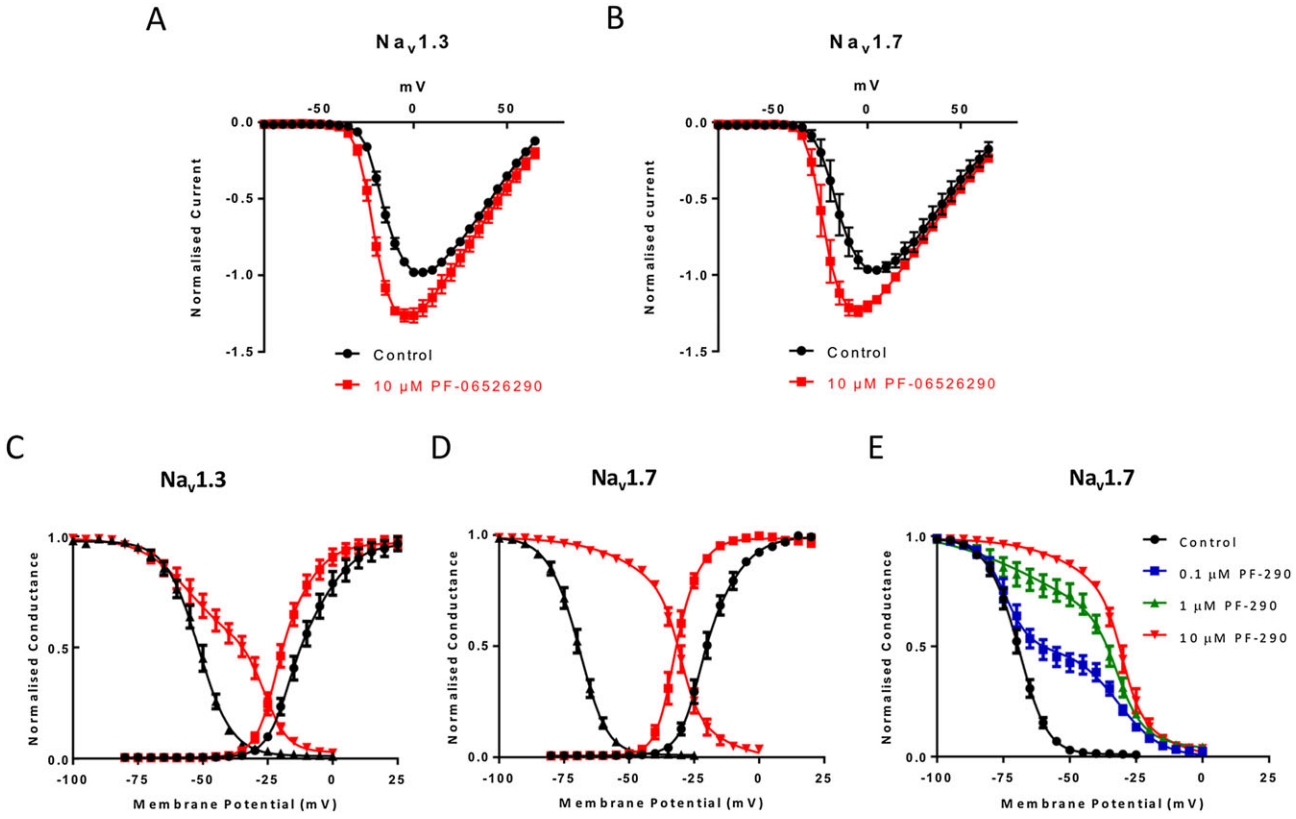

Figure 4

Effect of PF-06526290 on voltage dependence of activation and inactivation of $Na_v1.3$ and $Na_v1.7$ channels. (A, B) Normalized peak current amplitude versus stimulating voltage, for $hNa_v1.3$ and $hNa_v1.7$ channels in the absence and presence of 10 μM PF-06526290. Control currents were normalized to maximum current amplitude in the absence of PF-06526290, while compound effect on current amplitude for each cell was normalized to the maximal control current for that cell. Data shown are mean ± SEM for four to five separate cell recordings. (C, D) Voltage dependence of activation and inactivation of $Na_v1.3$ and $Na_v1.7$ channels in the absence and presence of 10 μM PF-06526290. Normalized conductance in the presence of PF-06526290 was measured 5 ms after peak current. [$hNa_v1.3$: Activation $V_{1/2}$: −12 ± 1, k: 7 ± 1.0 (n = 5); inactivation $V_{1/2}$: −52 ± 1, k: 6 ± 1 (n = 5); With 10 μM PF-06526290: Activation $V_{1/2}$: −19 ± 1, k: 6 ± 1 (n = 5); Inactivation $V_{1/2}$: −37 ± 2, k: 13 ± 2 (n = 5). $hNa_v1.7$: Activation $V_{1/2}$: −20 ± 1, k: 6 ± 1 (n = 4); Inactivation $V_{1/2}$: −70 ± 0.6, k: 6 ± 0.5 (n = 5); With 10 μM PF-06526290: Activation $V_{1/2}$: −32 ± 1, k: 6 ± 1 (n = 3); Inactivation $V_{1/2}$: −32 ± 1, k: 6 ± 1) (n = 6)]. Data generated from two separate cell preparations. (E) Voltage dependence of inactivation of $Na_v1.7$ in the presence of 0.1, 1 and 10 μM PF-06526290 (n = 5–6 cells from two separate cell preparations). Each data set was fitted to a double Boltzmann Equation where each of the $V_{1/2}$ and slope of inactivation parameters were fixed to either the control or 10 μM PF-06526290 values shown in (D). However, the relative proportion of current with either the −70 or −32 mV $V_{1/2}$ was adjusted to give the best fit for each concentration of PF-06526290 tested.

Furthermore, the time course for the redevelopment of slowed inactivation at the highest concentration tested (10 μM) was similar to the time course of the slow component of recovery from inactivation (Figure 6F).

Slowing of inactivation and inhibition by PF-06526290 result from distinct interactions with the channel

While the explanation in the previous section can mechanistically account for the loss of slowed inactivation of both $Na_v1.7$ and $Na_v1.3$ channels following sustained depolarization in the presence of PF-06526290, it does not account for the subtype-selective inhibition of $Na_v1.3$ channels, which appears to be dependent on prolonged depolarization. The structure of PF-06526290 includes a thiazole motif which is also present in the aryl sulfonamide class of subtype-selective inhibitors that have been shown to interact with the domain 4 voltage sensor domain (D4 VSD) of the sodium channel (McCormack *et al.*, 2013; Ahuja *et al.*, 2015; Alexandrou *et al.*, 2016). To evaluate if the functional effects of PF-06526290 resulted from an interaction with this region of the sodium channel, we examined the effect of previously characterized mutant forms of $Na_v1.3$ and $Na_v1.7$ channels where a 3 amino residue motif termed M123 swapped residues found in $Na_v1.3$ with those present in $Na_v1.7$ channels ($Na_v1.3$ M123 – S1510Y/R1511W/E1559D) or *vice versa* for $Na_v1.7$ ($Na_v1.7$ M123 -Y1537S/W1538R/D1586E) (McCormack *et al.*, 2013). Figure 7A compares the concentration dependence of PF-06526290-mediated inhibition of $Na_v1.3$, $Na_v1.7$ and the respective $Na_v1.3$/$Na_v1.7$ M123 domain 4 voltage sensor mutants. The potency of inhibition of $Na_v1.3$ M123 was decreased eightfold relative to $Na_v1.3$ channels while inhibition of $Na_v1.7$ M123 was

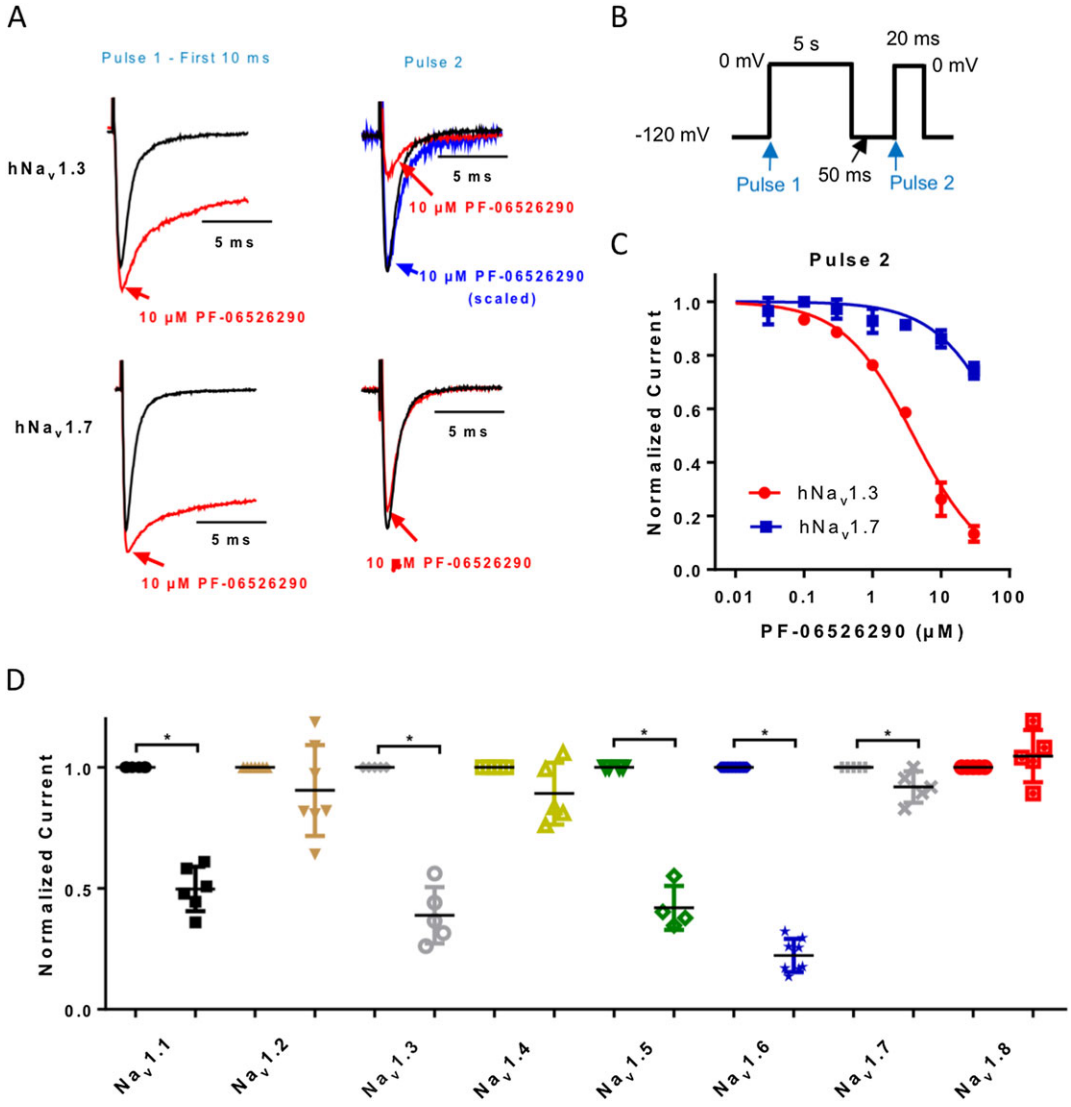

Figure 5

PF-06526290 produces subtype-selective inhibition of Na_v channels following prolonged depolarization. (A) Comparison of PF-06526290 effects on $Na_v1.3$ and $Na_v1.7$ current traces elicited by protocol shown in (B). Whereas slowing of inactivation by 10 µM PF-06526290 is observed for both channel subtypes with Pulse 1 only inhibition of $Na_v1.3$ current was observed with Pulse 2. Furthermore, neither $Na_v1.7$ nor $Na_v1.3$ current traces elicited by Pulse 2 exhibited the slowing of inactivation observed with Pulse 1 (for $Na_v1.3$, the blue trace reflects the uninhibited component scaled to control). (C) Concentration dependence of human $Na_v1.3$ and $Na_v1.7$ inhibition by PF-06526290 [IC_{50} 5 ± 2 µM (n = 6 cells from two cell preparations) for $Na_v1.3$ channels and > 30 µM (n = 6 cells from two cell preparations) for $Na_v1.7$ channels]. (D) Inhibition effect of PF-06526290 on different Na_v channel subtypes tested. For each sodium channel subtype, data before (left-hand data set) and after (right-hand data set) application of 10 µM PF-06526290 are shown. *$P < 0.05$; significantly different as indicated; Student's t-test.

enhanced sevenfold relative to $Na_v1.7$ channels, suggesting that the D4 VSD region may be involved this action. In contrast, Figure 7B shows that the mutation of $Na_v1.3$ or $Na_v1.7$ M123 residues had no obvious effect on the potency or magnitude of slowing of inactivation of either $Na_v1.3$ or $Na_v1.7$ channels. The absence of a change in magnitude or potency for slowing of inactivation with either $Na_v1.3$ M123 or $Na_v1.7$ M123 mutants may be explained by the fact that both $Na_v1.3$ and $Na_v1.7$ channels are sensitive to the inactivation slowing actions of PF-06526290. Therefore, swapping $Na_v1.3$ for $Na_v1.7$ residues or *vice versa* in the $Na_v1.3$ M123 and $Na_v1.7$ M123 mutants may have resulted in channels similarly sensitive to slowing of inactivation by PF-06526290.

The slowing of inactivation by PF-06526290 resembled the actions of scorpion venom α toxins and sea anemone toxins which have been reported to bind to the Na_v channel domain 4 voltage sensor (Leipold *et al.*, 2004; Gilchrist *et al.*, 2014). Furthermore, at least one of the residues in the M123 motif important for inhibition by PF-06526290 is important for α-scorpion toxin action (Leipold *et al.*, 2004; Gilchrist *et al.*, 2014). Therefore, we evaluated if PF-06526290 could modulate the ability of α-scorpion toxin to slow $Na_v1.7$ channel inactivation. The effect of the

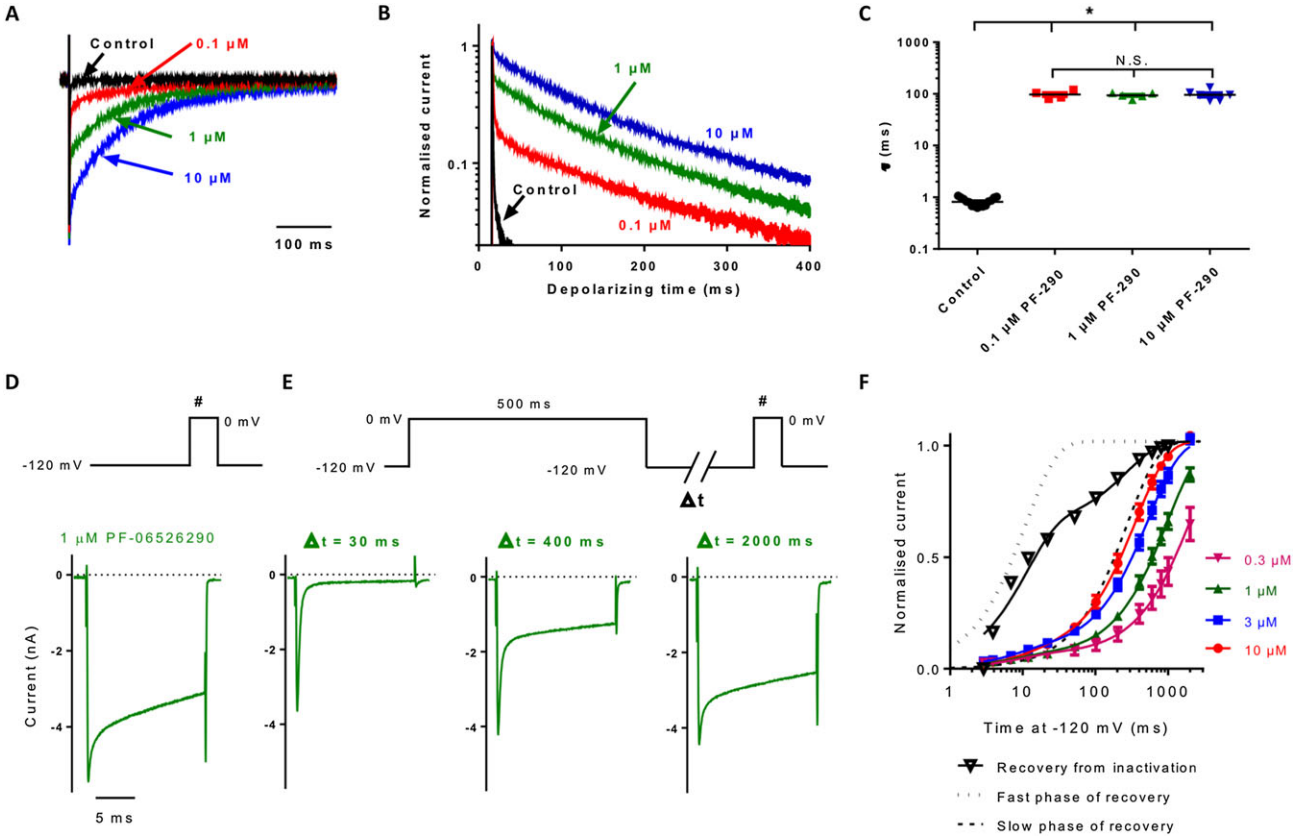

Figure 6

Properties of PF-06526290 induced slowing of Na_v channel inactivation. (A) Current traces of $Na_v1.7$ channels in the absence and presence of 0.1, 1 and 10 μM PF-06526290. Sodium currents were elicited by voltage steps to 0 mV for 500 ms from a holding potential of −120 mV (current amplitudes are normalized to peak for each trace). (B) Same sodium current traces from (A) normalized to peak and plotted on a log scale. (C) Time constant of inactivation (τ) in the absence and presence of 0.1, 1 and 10 μM PF-06526290 (n = 4–7 cells from four cell preparations). Current decay was fit with a single exponential. There was no significant difference between the calculated time constants for slow phase of inactivation at different concentrations of PF-06526290. *$P < 0.05$, significantly different from control; One way ANOVA with Tukey's *post hoc* test (D) $Na_v1.7$ current trace evoked by a single pulse depolarization to 0 mV for 20 ms from a holding potential of −120 mV the in presence of 1 μM PF-06526290. (E) Current traces elicited by the voltage protocol shown in the presence of 1 μM PF-06526290. A 500 ms depolarizing voltage step to 0 mV was applied to functionally displace PF-06526290. A rest period at −120 mV of variable duration was applied prior to a 20 ms test pulse (indicated by #) to assess fraction of current exhibiting slowed inactivation. (F) Concentration dependence of time course for recovery of slowed inactivation after 500 ms voltage step to 0 mV in the presence of PF-06526290. The I_{5ms}/I_{peak} current amplitude ratios determined during the test pulse (#) are plotted against time at −120 mV after 500 ms voltage step to 0 mV. $\tau_{Recovery}$ was determined from a least squares fit of a double exponential with the slow phase contributing 92–94% of the recovery for each concentration and τ_{slow} being 2311 ± 18 ms (n = 6), 994 ± 121 ms (n = 6) 540 ± 72 ms (n = 6) and 363 ± 63 ms (n = 5) for 0.3, 1, 3 and 10 μM PF-06526290 respectively. For comparison, the time course for recovery of $Na_v1.7$ inactivation following a 500 ms voltage step to 0 mV in the absence of PF-06526290 is also shown (Control). Data were fit with a double exponential with τ_{fast} = 11 ± 2, τ_{slow} = 270 ± 128 ms and fast/slow ratio of 0.74. Results shown in (D–F) were obtained using Molecular Devices PatchXpress automated patch clamp platform.

α-like scorpion toxin, Lqh III, which has been reported to slow inactivation of $Na_v1.7$ (Chen *et al.*, 2002) alone and in combination with 1 μM PF-06526290, is shown in Figure 7C. Application of 300 nM Lqh III slowed $Na_v1.7$ channel inactivation (τ_{inact} = 10 ± 1 ms compared to τ_{inact} = 0.8 ± 0.1 ms for control). However, the slowing was approximately 10-fold less than observed with 1 μM PF-06526290 (τ_{inact} = 96 ± 9 ms). If PF-06526290 and Lqh III interacted at the same or overlapping binding site, we would expect competition and thus the rate inactivation in the presence of both agents would be predicted to faster than PF-06526290 alone and slower than Lqh III alone. However, when both 300 nM Lqh III and 1 μM PF-06526290 were applied in combination, $Na_v1.7$ inactivation was further slowed to τ_{inact} = 1100 ± 64 ms (Figure 7C, D). The synergistic actions of co-administered Lqh III and PF-06526290 suggest independent but functionally coupled interactions with the channel.

It is known that other enhancers ("activators") of Na_v channel conduction like batrachotoxin, veratridine and pyrethroids interact with the region near or overlapping with the canonical local anaesthetic binding site on the D4 S6 transmembrane segment of the pore (Ragsdale *et al.*, 1994; Ragsdale *et al.*, 1996; Son *et al.*, 2004). Therefore, we

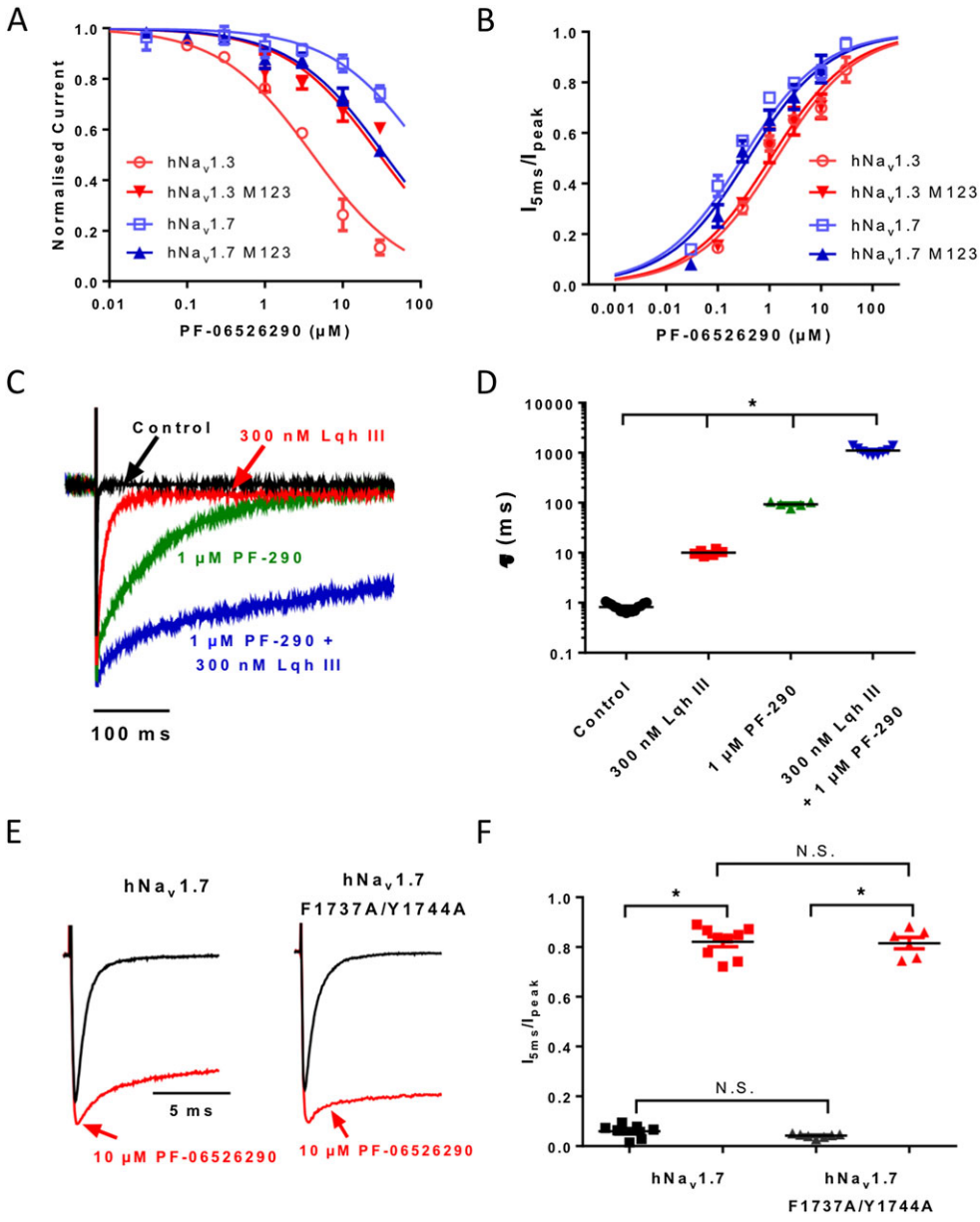

Figure 7

(A) Introduction of M123 (S1510Y/R1511W/E1559D) residues into $Na_v1.7$ increases sensitivity to inhibition by PF-06526290 whereas introduction of M123 (Y1537S/W1538R/D1586E) residues into $Na_v1.3$ reduces its sensitivity to inhibition by PF-06526209 [IC_{50}: 5 ± 2 μM (n = 6 cells) for $Na_v1.3$, 30 ± 5 μM (n = 3 cells) for $Na_v1.3$ M123, >100 μM (n = 6 cells) for $Na_v1.7$ and 35 ± 4 μM (n = 3 cells) for $Na_v1.7$ M123] (from at least two separate cell preparations). (B) Mutation of M123 residues has no effect on PF-06526290-induced slowing of inactivation in either $Na_v1.3$ or $Na_v1.7$ [EC_{50}: 1.1 ± 0.1 μM (n = 5 cells) for $Na_v1.3$, 1.1 ± 0.4 μM (n = 4 cells) for $Na_v1.3$ M123, 0.27 ± 0.08 μM (n = 6 cells) for $Na_v1.7$, and 0.39 ± 0.13 μM (n = 3 cells) for $Na_v1.7$ M123] (from at least two separate cell preparations). (C) $Na_v1.7$ current traces recorded in the presence of 300 nM scorpion toxin Lqh III, 1 μM PF-06526290 (PF-290) or mixture of 300 nM Lqh III + 1 μM PF-06526290. Currents were elicited by a 5 s voltage step from −120 to 0 mV (traces show the first 500 ms). (D) Plot of inactivation time constants (τ_{inact}) in the absence and presence of 300 nM Lqh III (n = 6), 1 μM PF-06526290 (PF-290) (n = 5) or a mixture of 300 nM Lqh III + 1 μM PF-06526290 (n = 9). τ_{inact} was determined from a fit of a single exponential equation. Data derived from three separate cell preparations. *$P < 0.05$, significantly different from control; One way ANOVA with Tukey's *post hoc* test. (E) Current traces comparing effect of 10 μM PF-06526290 on inactivation of $Na_v1.7$ versus the local anaesthetic binding site mutant $Na_v1.7$ F1737A/Y1744A. (F) Plot of I_{5ms}/I_{peak} current amplitude ratio for both $Na_v1.7$ and $Na_v1.7$ F1737A/Y1744A in the presence and absence of 10 μM PF-06526290 Data shown are from six to nine separate experiments. *$P < 0.05$, significantly different as indicated; N.S., not significant; One way ANOVA with Tukey's *post hoc* test.

examined the effect of 10 μM PF-06526290 on a $Na_v1.7$ F1737A/Y1744A mutant, which we have previously shown to decrease local anaesthetic potency by >100-fold (McCormack *et al.*, 2013). Figure 7E, F shows that no reduction in PF-06526290-induced slowing of inactivation was observed with $Na_v1.7$ F1737A/Y1744A suggesting that this

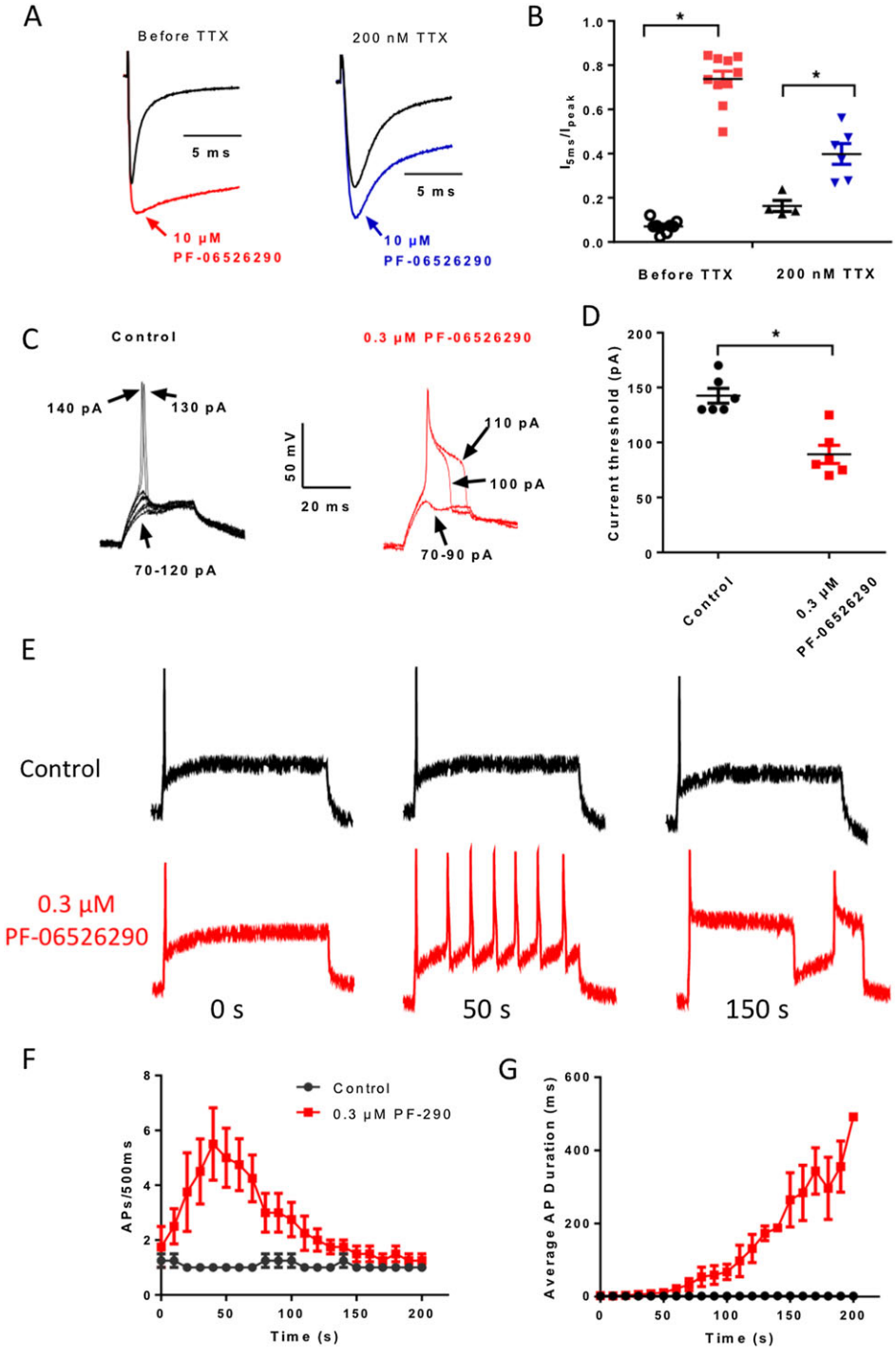

Figure 8

PF-06526290 slows inactivation of endogenous Na_v currents and increases neuronal excitability in mouse sensory neurons. (A) Sodium current traces showing the slowing of inactivation by 10 μM PF-06526290 in the absence or presence of 200 nM TTX to isolate the TTX-resistant component. Sodium currents were elicited by a single pulse test to 0 mV for 20 ms from a holding potential of −120 mV. (B) Plot of the I_{5ms}/I_{peak} current amplitude ratio for TTX-sensitive and -resistant currents in the presence of 10 μM PF-06526290 (n = 8–10 neurons recorded over 3 days from two separate cell isolations). *$P < 0.05$, significantly different as indicated; N.S., not significant; One way ANOVA with Tukey's *post hoc* test. (C) Effect of 0.3 μM PF-06526290 on stimulus intensity (current injection in pA) required to initiate action potential. (D) Plot of current injection threshold for initiation of action potential in the presence and absence of 0.3 μM PF-06526290 (n = 6 neurons recorded over 3 days from two separate cell isolations). *$P < 0.05$, significantly different as indicated; N.S., not significant; Student's t-test. (E) Time-dependent change in number of action potentials elicited by a 500 ms 150 pA supramaximal stimulus at 0.1 Hz in the absence or following administration of 0.3 μM PF-06526290. Plot time course of action potential frequency (F) or duration at 50% repolarization (G), in the absence or following administration 0.3 μM PF-06526290 using stimulus protocol used in (E) (n = 6 neurons recorded over 2 days from two separate cell isolations).

region of the channel is probably not involved in PF-06526290's conduction enhancing actions.

PF-06526290 slows inactivation of native Na_v currents and increases excitability in sensory neurons

Slowing of Na_v channel inactivation by scorpion and anemone toxins are associated with increased neuronal excitability (Benoit and Gordon, 2001; Yamaji *et al.,* 2009). To determine if the PF-06526290 produces a similar effect, we examined its actions on mouse DRG sodium currents and action potential properties. PF-06526290 slowed inactivation of both TTX-sensitive and -resistant sodium currents in mouse DRG neurons (Figure 8A, B). PF-06526290 at 10 μM was applied in the absence and presence of 200 nM TTX used to isolate TTX-resistant component. In the absence of TTX, 10 μM PF-06526290 slowed inactivation such that current amplitude 5 ms after start of depolarizing voltage step was 76 ± 3% of peak versus 8 ± 1% for control currents (Figure 8B). In the presence of 200 nM TTX, slowing of inactivation was less profound (I_{5ms}/I_{peak} = 42 ± 5% vs. 17 ± 3% for control) but was similar in profile and magnitude to that seen with recombinant $Na_v1.8$ currents (Figure 3E).

Figure 8C–G shows the effect of PF-06526290 on mouse DRG neuron excitability. In the presence of 0.3 μM PF-06526290, the action potential threshold was reduced (Figure 8C, D). Using a supramaximal 500 ms stimulation of 150 pA to evoke action potential firing, 0.3 μM PF-06526290 initially increased the frequency of action potential firing, which progressed to prolongation of action potential duration with APD_{50} > 400 ms after 3 min of exposure (Figure 8E–G).

To test the possibility that prolongation of action potential duration by PF-06526290 may be due in part to inhibition of potassium channels, we examined the effect of the agent on the neuronal delayed rectifier $K_v1.1/1.2$ channels. No inhibition by PF-06526290 was observed up to 10 μM (Supporting Information Figure S1).

Discussion

The present study has focused on expanding our understanding of modulation of Na_v channels by a new agent that exhibits both inhibition and enhancement of current flow. PF-06526290 greatly slows inactivation, which occurs with all Na_v channel subtypes examined. PF-06526290 also slows inactivation of TTX-sensitive and -resistant Na_v currents in mouse sensory neurons, which is associated with action potential prolongation and increased frequency of firing similar to that observed with scorpion and anemone toxins, which also slow Na_v channel inactivation (Benoit and Gordon, 2001; Abbas *et al.,* 2013).

In contrast to its ability to slow inactivation, which appears to result from an interaction with closed channels, PF-06526290 was found to selectively inhibit $Na_v1.3$ rather than $Na_v1.7$ channels *via* an apparent preferential interaction with inactivated state(s) of the channel. Similarly, the switching of $Na_v1.3$ to $Na_v1.7$ selectivity *via* the mutation of the M123 motif suggests that inhibition might be mediated *via* an interaction with the homologous domain 4 voltage sensor. The magnitude of the M123 motif mutation-induced modulation of the inhibitory effects of PF-06526290 is less than reported for aryl sulfonamide inhibitors like PF-04856264 and PF-05089771 (McCormack *et al.,* 2013; Alexandrou *et al.,* 2016). However, this may reflect the involvement of other residues for interaction, especially given the structural differences between these classes of molecule. The involvement of other residues beyond M123 motif for aryl sulfonamide $Na_v1.7$ channel inhibitors has also been described (McCormack *et al.,* 2013; Ahuja *et al.,* 2015). Alternatively, the shifts in potency observed with the $Na_v1.7$ M123 mutation may reflect an indirect effect of modulating the voltage-gating process which is translated to other regions of the channels that may be the site of PF-06526290 interaction.

The Na_v channel subtype-independent slowing of inactivation observed with PF-06526290 appears to result from an interaction with resting closed state(s) (and possibly open states). Although inactivation of Na_v channels is slowed in the presence of PF-06526290, prolonged depolarization (>500 ms) eventually results in inactivation reaching completion, and the rate at which this is achieved is independent of concentration applied. This finding can be interpreted as PF-06526290 interaction leads to inhibition of fast inactivation to expose a slower inactivation process that is not affected by it. Our observation that PF-06526290 does not produce a concentration-dependent shift in the voltage dependence of inactivation but rather increases the proportion of channels that inactivate with a more depolarized midpoint potential (−32 vs. −70 mV for unmodified channels) is consistent with this hypothesis. We also found that the establishment of slowed inactivation results in the functional displacement of PF-06526290 from the channel despite its continued presence and re-interaction only occurs after the channels return to the resting closed state.

While the functional displacement of PF-06526290 was most evident with $Na_v1.7$ channels (due to the absence of an inhibitory effect), it was also observed with the non-inhibited component of $Na_v1.3$ channels, suggesting that resting state-dependent slowing of inactivation and inactivated state-dependent inhibition are functionally distinct processes. Finally, while the inhibitory actions of PF-06526290 is modulated by M123 motif mutation of domain 4 VSD, these mutations had no effect on slowing of inactivation of either $Na_v1.3$ or $Na_v1.7$ channels. It can be noted that the absence of effect of M123 motif mutation on PF-06526290-induced slowing of inactivation does not exclude the possibility that this effect is still mediated *via* an interaction with the domain 4 VSD, as the mutations swapped $Na_v1.3$ for $Na_v1.7$ residues or *vice versa*, and both channel subtypes exhibit a slowed inactivation in the presence of this modulator.

Homologous domain 4 VSD has been shown to be the site of interaction for scorpion and anemone peptide toxins, which, like PF-06526290, cause slowing of inactivation of Na_v channels (Rogers *et al.,* 1996; Leipold *et al.,* 2004; Billen *et al.,* 2008; Wang *et al.,* 2011; Gilchrist *et al.,* 2014; Martin-Eauclaire *et al.,* 2015). Interestingly, site 3 scorpion α and anemone toxins achieve their modulation of inactivation *via* an interaction with amino acid residues that include the third residue of the M123 motif (E1559 on $Na_v1.3$ and D1586 on $Na_v1.7$) (Rogers *et al.,* 1996; Leipold *et al.,* 2004;

Wang *et al.,* 2011; Gurevitz, 2012; Gilchrist *et al.,* 2014). Given the similar mode of channel modulation and preference for resting state channels, as well as the overlap of D4 VSD regions important for toxin action and the inhibitory effects of PF-06526290, we explored possible interaction of the α-like toxin Lqh3 with PF-06526290. If the two agents interact with a common site, we would expect that the time course of slowing of inactivation when the Lqh3 and PF-06526290 are applied together would be somewhere between the time courses observed with each agent applied individually. In contrast to this expectation, inactivation was slowed a further 10-fold, suggesting synergism between Lqh3 and PF-06526290. This implies that Lqh3 and PF-06526290 have functionally coupled but distinct interactions with the channel. However, as with the M123 mutations, these findings do not exclude the possibility that the slowed inactivation still results from an interaction with the D4 VSD.

We did explore the possibility that PF-06526290 might interact with the local anaesthetic binding site within the pore since a number of Na_v channel activators like veratridine are reported to interact with or near this region of the channel (Son *et al.,* 2004; Tikhonov and Zhorov, 2005; Yoshinaka-Niitsu *et al.,* 2012). However, we found that mutation of the local anaesthetic binding site on $Na_v1.7$ site did not prevent PF-06526290-mediated slowing of inactivation, suggesting that this region is probably not involved in the interaction producing this effect.

Currently, the region of the sodium channel responsible for PF-06526290-induced slowing of inactivation remains elusive. We have not been able to exclude the possibility that the effect is mediated *via* an interaction with the domain 4 VSD, so future studies directed towards investigating the potential role of other residues in the region may help in this regard. Of course, there remains the possibility that the site of interaction mediating the slowed inactivation is located elsewhere, including other VSDs. We have shown that the magnitude of slowing of inactivation of $Na_v1.4$ and $Na_v1.8$ channels is considerably less than that observed with the other Na_v channel subtypes. It may be possible to exploit these differences in future studies to construct homologous domain swap chimeras to home in on potential regions of interaction in a manner similar to that successfully employed to identify the D4 VSD interaction site for selective inhibitors (McCormack *et al.,* 2013). Potential guidance can also come from examining previously characterized agents which have both enhancing and inhibitory effects. For example, the dual inhibition and slowing of voltage-dependent sodium channel inactivation has also been reported for the cardiac inotropic agent DPI 201-106 (Romey *et al.,* 1987; Wang *et al.,* 1990). The (S)-enantiomer of DPI 201-106 slows inactivation whereas the (R)-enantiomer inhibits Na_v channel function. The exact location on the channel mediating these effects remains to be reported, although a detailed study by Wang *et al.* (1990) did provide evidence that slowing of inactivation and inhibition was mediated by separate non-overlapping interactions with the channel. The enantiomer-dependent effects of DPI 201-106 are reminiscent of the voltage-dependent calcium channel inhibition/activation elicited by enantiomers of dihydropyridines (Hockerman *et al.,* 1997; Natale and Steiger, 2014) which have been reported to result from interactions with the homologous domains 3 and 4 S5 and S6 transmembrane helices that form the pore (Peterson *et al.,* 1996; Hockerman *et al.,* 1997; Schleifer, 1999). Similar inhibition/activation switching has been reported for modulators of TRPA1 and potassium channels as well as agonist/inverse agonists of GABA receptor channels (Ferretti *et al.,* 2004; Defalco *et al.,* 2010; Banzawa *et al.,* 2014).

In conclusion, the findings from the current study have shown that a single agent, PF-06526290, can exhibit both enhancement and inhibition of sodium channel function. This dual mode of Na_v channel modulation likely results from distinct interactions with the channel. The ability of PF-06526290 to interact with distinct gating states to elicit opposing effects on conduction may make it a useful tool for further understanding how pharmacological modulation of gating leads to conduction changes.

Although much of the historical focus on developing drug candidates targeting voltage-dependent sodium channels has been directed towards inhibitors, there has recently been increased interest in developing agents that can enhance sodium channel function/conduction. Seizure and autism spectrum disorders associated with human loss of function mutations of $Na_v1.1$, $Na_v1.2$, $Na_v1.3$ and $Na_v1.6$ channels may benefit from pharmacological enhancement of channel conduction. Therefore, improved understanding of the site of action of agents like PF-06526290 may provide opportunities to develop more subtype-selective enhancers of Na_v channels, which in turn could provide new treatment options for rare epilepsies and other neurological disorders like autism.

Acknowledgements

Lingxin Wang was the recipient of a Pfizer Worldwide Research and Development Postdoctoral Fellowship. The authors would like to thank Sally Stoehr and Peter Miu for help with initial experiments; Christopher West and Wes Ergle for synthesizing PF-06526290; Joseph Warmus and Ivan Samardjiev for analysis and determination of PF-06526290 structure; Sonia Santos for constructing $Na_v1.3$ and $Na_v1.7$ M123 mutants; Eva Prazak and Doug McIlvaine for providing cells; and Mark Chapman and Doug Krafte for their suggestions during the drafting of the manuscript.

Author contributions

L.W., S.G.Z. and D.M.P. performed the research. L.W. and N.A.C. designed the research. L.W. and N.A.C. analysed the data. L.W. and N.A.C. wrote the manuscript.

Conflict of interest

Lingxin Wang, Shannon G. Zellmer, David M. Printzenhoff and Neil A. Castle were employees of Pfizer at the time the studies were performed. Pfizer is the developer of PF-06526290. Research was conducted on human tissue acquired from a third party that has been verified as compliant with Pfizer policies, including IRB/IEC approval.

Declaration of transparency and scientific rigour

This Declaration acknowledges that this paper adheres to the principles for transparent reporting and scientific rigour of preclinical research recommended by funding agencies, publishers and other organisations engaged with supporting research.

References

Abbas N, Gaudioso-Tyzra C, Bonnet C, Gabriac M, Amsalem M, Lonigro A *et al.* (2013). The scorpion toxin Amm VIII induces pain hypersensitivity through gain-of-function of TTX-sensitive Na(+) channels. Pain 154: 1204–1215.

Ahuja S, Mukund S, Deng L, Khakh K, Chang E, Ho H *et al.* (2015). Structural basis of Nav1.7 inhibition by an isoform-selective small-molecule antagonist. Science 350: aac5464.

Alexander SPH, Striessnig J, Kelly E, Marrion NV, Peters JA, Faccenda E *et al.* (2017). The Concise Guide to PHARMACOLOGY 2017/18: Voltage-gated ion channels. Br J Pharmacol 174: S160–S194.

Alexandrou AJ, Brown AR, Chapman ML, Estacion M, Turner J, Mis MA *et al.* (2016). Subtype-selective small molecule inhibitors reveal a fundamental role for Nav1.7 in nociceptor electrogenesis, axonal conduction and presynaptic release. PLoS One 11: e0152405.

Bagal SK, Bungay PJ, Denton SM, Gibson KR, Glossop MS, Hay TL *et al.* (2015). Discovery and optimization of selective Nav1.8 modulator series that demonstrate efficacy in preclinical models of pain. ACS Med Chem Lett 6: 650–654.

Banzawa N, Saito S, Imagawa T, Kashio M, Takahashi K, Tominaga M *et al.* (2014). Molecular basis determining inhibition/activation of nociceptive receptor TRPA1 protein: a single amino acid dictates species-specific actions of the most potent mammalian TRPA1 antagonist. J Biol Chem 289: 31927–31939.

Bennett DL, Woods CG (2014). Painful and painless channelopathies. Lancet Neurol 13: 587–599.

Benoit E, Gordon D (2001). The scorpion alpha-like toxin Lqh III specifically alters sodium channel inactivation in frog myelinated axons. Neuroscience 104: 551–559.

Bezanilla F (2006). The action potential: from voltage-gated conductances to molecular structures. Biol Res 39: 425–435.

Billen B, Bosmans F, Tytgat J (2008). Animal peptides targeting voltage-activated sodium channels. Curr Pharm Des 14: 2492–2502.

Black JA, Waxman SG (2013). Noncanonical roles of voltage-gated sodium channels. Neuron 80: 280–291.

Blanchard MG, Willemsen MH, Walker JB, Dib-Hajj SD, Waxman SG, Jongmans MC *et al.* (2015). De novo gain-of-function and loss-of-function mutations of SCN8A in patients with intellectual disabilities and epilepsy. J Med Genet 52: 330–337.

Castle NA, Wickenden AD, Zou A (2003). Electrophysiological analysis of heterologously expressed Kv and SK/IK potassium channels. Current Protocols in Pharmacology/Editorial Board, SJ Enna (editor-in-chief) [et al] Chapter 11**:** Unit11.15.

Catterall WA (2012). Voltage-gated sodium channels at 60: structure, function and pathophysiology. J Physiol 590: 2577–2589.

Chen H, Lu S, Leipold E, Gordon D, Hansel A, Heinemann SH (2002). Differential sensitivity of sodium channels from the central and peripheral nervous system to the scorpion toxins Lqh-2 and Lqh-3. Eur J Neurosci 16: 767–770.

Crestey F, Frederiksen K, Jensen HS, Dekermendjian K, Larsen PH, Bastlund JF *et al.* (2015). Identification and electrophysiological evaluation of 2-methylbenzamide derivatives as Nav1.1 modulators. ACS Chem Nerosci 6: 1302–1308.

Cummins TR, Sheets PL, Waxman SG (2007). The roles of sodium channels in nociception: Implications for mechanisms of pain. Pain 131: 243–257.

Curtis MJ, Bond RA, Spina D, Ahluwalia A, Alexander SP, Giembycz MA *et al.* (2015). Experimental design and analysis and their reporting: new guidance for publication in BJP. Br J Pharmacol 172: 3461–3471.

Defalco J, Steiger D, Gustafson A, Emerling DE, Kelly MG, Duncton MA (2010). Oxime derivatives related to AP18: agonists and antagonists of the TRPA1 receptor. Bioorg Med Chem Lett 20: 276–279.

Eijkelkamp N, Linley JE, Baker MD, Minett MS, Cregg R, Werdehausen R *et al.* (2012). Neurological perspectives on voltage-gated sodium channels. Brain 135: 2585–2612.

England S, de Groot MJ (2009). Subtype-selective targeting of voltage-gated sodium channels. Br J Pharmacol 158: 1413–1425.

Ferretti V, Gilli P, Borea PA (2004). Structural features controlling the binding of beta-carbolines to the benzodiazepine receptor. Acta Crystallogr B 60: 481–489.

Fozzard HA, Sheets MF, Hanck DA (2011). The sodium channel as a target for local anesthetic drugs. Front Pharmacol 2: 68.

Gandini MA, Sandoval A, Felix R (2014). Whole-cell patch-clamp recordings of Ca2+ currents from isolated neonatal mouse dorsal root ganglion (DRG) neurons. Cold Spring Harb Protoc 2014: 389–395.

Gilchrist J, Olivera BM, Bosmans F (2014). Animal toxins influence voltage-gated sodium channel function. Handb Exp Pharmacol 221: 203–229.

Gurevitz M (2012). Mapping of scorpion toxin receptor sites at voltage-gated sodium channels. Toxicon 60: 502–511.

Harding SD, Sharman JL, Faccenda E, Southan C, Pawson AJ, Ireland S *et al.* (2018). The IUPHAR/BPS Guide to PHARMACOLOGY in 2018: updates and expansion to encompass the new guide to IMMUNOPHARMACOLOGY. Nucl Acids Res 46: D1091–D1106.

Hockerman GH, Peterson BZ, Sharp E, Tanada TN, Scheuer T, Catterall WA (1997). Construction of a high-affinity receptor site for dihydropyridine agonists and antagonists by single amino acid substitutions in a non-L-type Ca2+ channel. Proc Natl Acad Sci U S A 94: 14906–14911.

Hodgkin AL, Huxley AF (1952). A quantitative description of membrane current and its application to conduction and excitation in nerve. J Physiol 117: 500–544.

Jarvis MF, Honore P, Shieh CC, Chapman M, Joshi S, Zhang XF *et al.* (2007). A-803467, a potent and selective Nav1.8 sodium channel blocker, attenuates neuropathic and inflammatory pain in the rat. Proc Natl Acad Sci U S A 104: 8520–8525.

Jensen HS, Grunnet M, Bastlund JF (2014). Therapeutic potential of Na(V)1.1 activators. Trends Pharmacol Sci 35: 113–118.

Kort ME, Drizin I, Gregg RJ, Scanio MJ, Shi L, Gross MF *et al.* (2008). Discovery and biological evaluation of 5-aryl-2-furfuramides, potent and selective blockers of the Nav1.8 sodium channel with efficacy in

models of neuropathic and inflammatory pain. J Med Chem 51: 407–416.

Krumm N, O'Roak BJ, Shendure J, Eichler EE (2014). A de novo convergence of autism genetics and molecular neuroscience. Trends Neurosci 37: 95–105.

Lamar T, Vanoye CG, Calhoun J, Wong JC, Dutton SB, Jorge BS *et al.* (2017). SCN3A deficiency associated with increased seizure susceptibility. Neurobiol Dis 102: 38–48.

Lee JH, Park CK, Chen G, Han Q, Xie RG, Liu T *et al.* (2014). A monoclonal antibody that targets a NaV1.7 channel voltage sensor for pain and itch relief. Cell 157: 1393–1404.

Leipold E, Lu S, Gordon D, Hansel A, Heinemann SH (2004). Combinatorial interaction of scorpion toxins Lqh-2, Lqh-3, and LqhalphaIT with sodium channel receptor sites-3. Mol Pharmacol 65: 685–691.

Martin-Eauclaire MF, Ferracci G, Bosmans F, Bougis PE (2015). A surface plasmon resonance approach to monitor toxin interactions with an isolated voltage-gated sodium channel paddle motif. J Gen Physiol 145: 155–162.

McCormack K, Santos S, Chapman ML, Krafte DS, Marron BE, West CW *et al.* (2013). Voltage sensor interaction site for selective small molecule inhibitors of voltage-gated sodium channels. Proc Natl Acad Sci U S A 110: E2724–E2732.

Miller D, Wang L, Zhong J (2014). Sodium channels, cardiac arrhythmia, and therapeutic strategy. Adv Pharmacol 70: 367–392.

Moreau A, Gosselin-Badaroudine P, Chahine M (2014). Biophysics, pathophysiology, and pharmacology of ion channel gating pores. Front Pharmacol 5: 53.

Natale NR, Steiger SA (2014). 4-isoxazolyl-1,4-dihydropyridines: a tale of two scaffolds. Future Med Chem 6: 923–943.

Panigel J, Cook SP (2011). A point mutation at F1737 of the human Nav1.7 sodium channel decreases inhibition by local anesthetics. J Neurogenet 25: 134–139.

Payne CE, Brown AR, Theile JW, Loucif AJ, Alexandrou AJ, Fuller MD *et al.* (2015). A novel selective and orally bioavailable Nav 1.8 channel blocker, PF-01247324, attenuates nociception and sensory neuron excitability. Br J Pharmacol 172: 2654–2670.

Peterson BZ, Tanada TN, Catterall WA (1996). Molecular determinants of high affinity dihydropyridine binding in L-type calcium channels. J Biol Chem 271: 5293–5296.

Ragsdale DS, McPhee JC, Scheuer T, Catterall WA (1994). Molecular determinants of state-dependent block of Na+ channels by local anesthetics. Science 265: 1724–1728.

Ragsdale DS, McPhee JC, Scheuer T, Catterall WA (1996). Common molecular determinants of local anesthetic, antiarrhythmic, and anticonvulsant block of voltage-gated Na+ channels. Proc Natl Acad Sci U S A 93: 9270–9275.

Rogers JC, Qu Y, Tanada TN, Scheuer T, Catterall WA (1996). Molecular determinants of high affinity binding of alpha-scorpion toxin and sea anemone toxin in the S3-S4 extracellular loop in domain IV of the Na+ channel alpha subunit. J Biol Chem 271: 15950–15962.

Romey G, Quast U, Pauron D, Frelin C, Renaud JF, Lazdunski M (1987). Na+ channels as sites of action of the cardioactive agent DPI 201-106 with agonist and antagonist enantiomers. Proc Natl Acad Sci U S A 84: 896–900.

Schleifer KJ (1999). Stereoselective characterization of the 1,4-dihydropyridine binding site at L-type calcium channels in the resting state and the opened/inactivated state. J Med Chem 42: 2204–2211.

Son SL, Wong K, Strichartz G (2004). Antagonism by local anesthetics of sodium channel activators in the presence of scorpion toxins: two mechanisms for competitive inhibition. Cell Mol Neurobiol 24: 565–577.

Sun S, Jia Q, Zenova AY, Chafeev M, Zhang Z, Lin S *et al.* (2014). The discovery of benzenesulfonamide-based potent and selective inhibitors of voltage-gated sodium channel Na(v)1.7. Bioorg Med Chem Lett 24: 4397–4401.

Tikhonov DB, Zhorov BS (2005). Sodium channel activators: model of binding inside the pore and a possible mechanism of action. FEBS Lett 579: 4207–4212.

Wang G, Dugas M, Ben Armah I, Honerjager P (1990). Interaction between DPI 201-106 enantiomers at the cardiac sodium channel. Mol Pharmacol 37: 17–24.

Wang J, Yarov-Yarovoy V, Kahn R, Gordon D, Gurevitz M, Scheuer T *et al.* (2011). Mapping the receptor site for alpha-scorpion toxins on a Na+ channel voltage sensor. Proc Natl Acad Sci U S A 108: 15426–15431.

Waxman SG, Merkies IS, Gerrits MM, Dib-Hajj SD, Lauria G, Cox JJ *et al.* (2014). Sodium channel genes in pain-related disorders: phenotype-genotype associations and recommendations for clinical use. Lancet Neurol 13: 1152–1160.

Wolff M, Johannesen KM, Hedrich UB, Masnada S, Rubboli G, Gardella E *et al.* (2017). Genetic and phenotypic heterogeneity suggest therapeutic implications in SCN2A-related disorders. Brain 140: 1316–1336.

Yamaji N, Little MJ, Nishio H, Billen B, Villegas E, Nishiuchi Y *et al.* (2009). Synthesis, solution structure, and phylum selectivity of a spider delta-toxin that slows inactivation of specific voltage-gated sodium channel subtypes. J Biol Chem 284: 24568–24582.

Yoshinaka-Niitsu A, Yamagaki T, Harada M, Tachibana K (2012). Solution NMR analysis of the binding mechanism of DIVS6 model peptides of voltage-gated sodium channels and the lipid soluble alkaloid veratridine. Bioorg Med Chem 20: 2796–2802.

Zhang XF, Shieh CC, Chapman ML, Matulenko MA, Hakeem AH, Atkinson RN *et al.* (2010). A-887826 is a structurally novel, potent and voltage-dependent Na(v)1.8 sodium channel blocker that attenuates neuropathic tactile allodynia in rats. Neuropharmacology 59: 201–207.

Supporting Information

Additional supporting information may be found online in the Supporting Information section at the end of the article.

https://doi.org/10.1111/bph.14338

Figure S1 Effect of PF-06526290 on voltage gated potassium currents.